Preliminary look at mesoscale dynamics of tropical cyclogenesis observed during PREDICT

Michael Bell and Michael Montgomery
Naval Postgraduate School
PREDICT Workshop 9 June 2010

Hypothesis 1: Tropical depression formation is greatly favored in the critical-layer region of the pre-depression wave or disturbance.

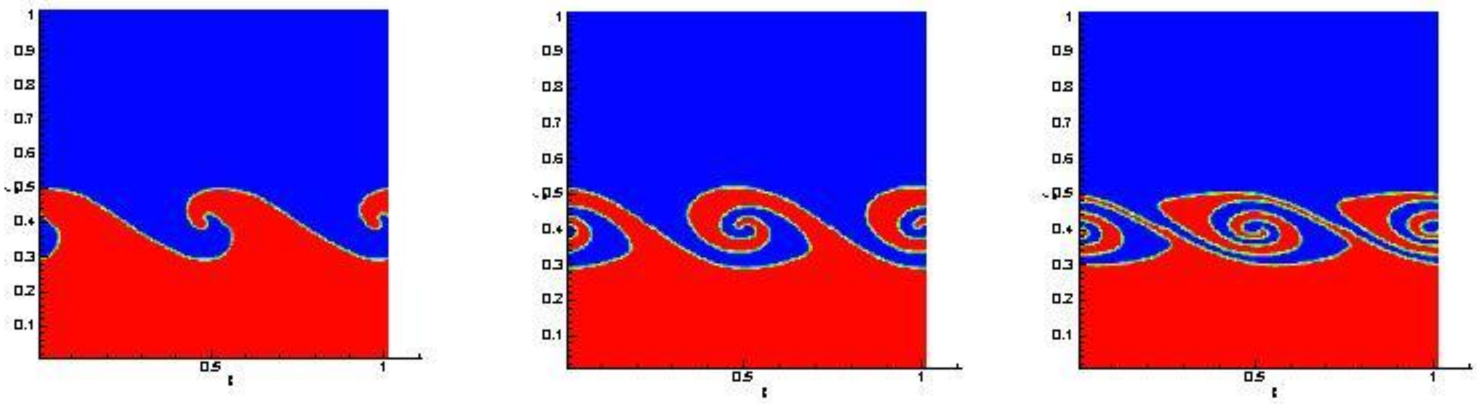

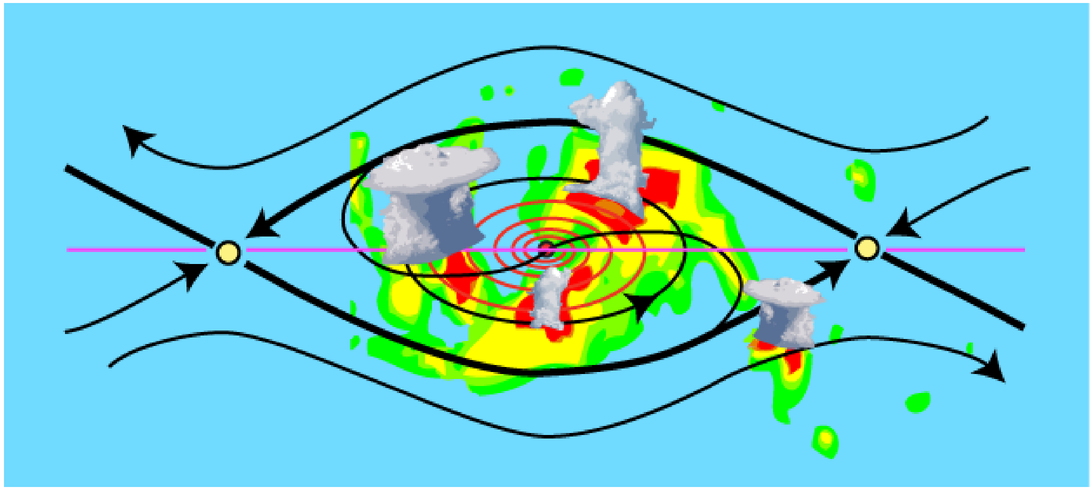

Dunkerton, Montgomery, and Wang (2009)

Hypothesis 2: Despite the variety of synoptic-scale precursors, tropical cyclone formation proceeds through essentially the same mesoscale and cloud processes.

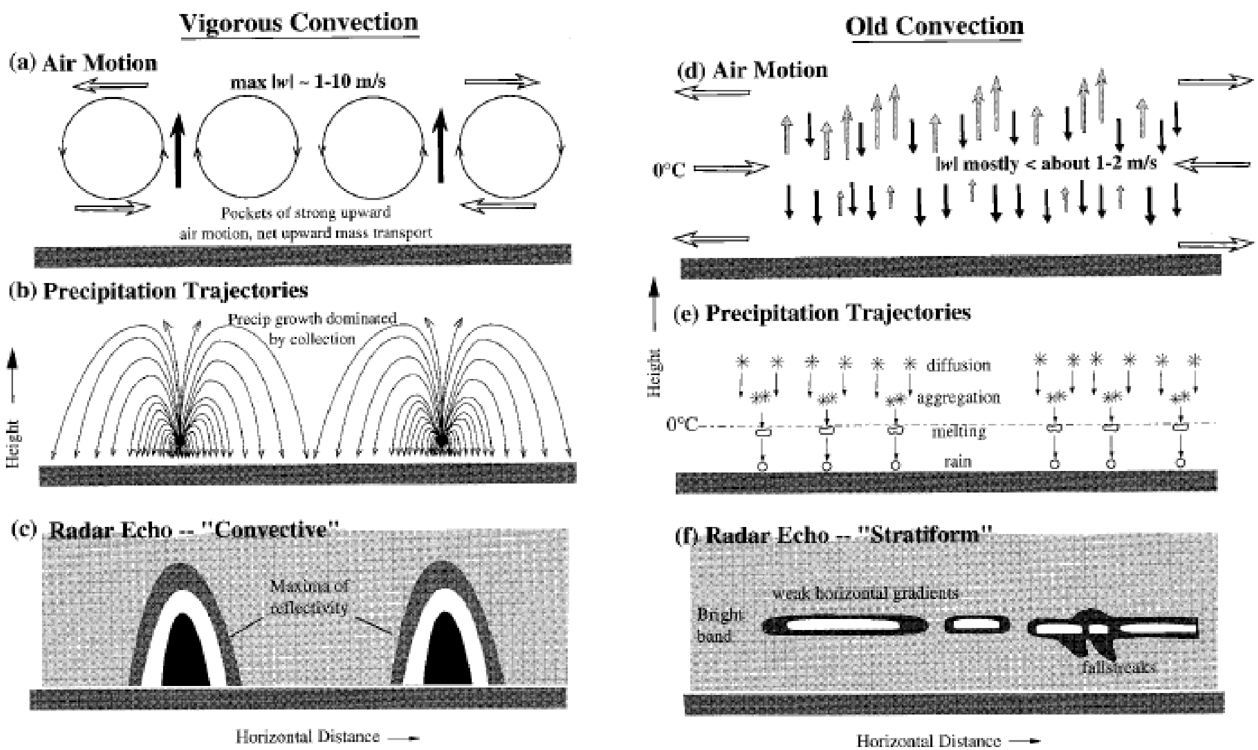

FIG. 1. Conceptual models of vertical cross sections through (a)–(c) young, vigorous precipitating convection and (d)–(f) old convection.

Convective

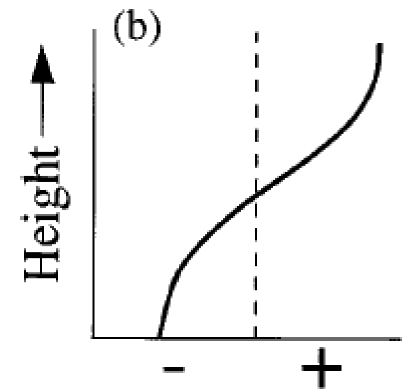

Stratiform

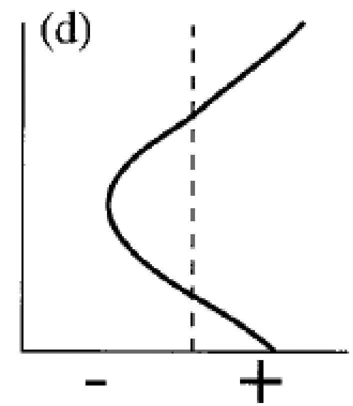

From Houze 1997

Hypothesis 3: Active deep convective regions are the primary contributors to low-level spin up

$$\frac{\partial C}{\partial t} = -\bar{\eta}\delta A - \oint \eta'\mathbf{v}' \cdot \hat{\mathbf{n}}\,dl + \oint w\left(\hat{\mathbf{k}} \times \frac{\partial \mathbf{V}}{\partial p}\right) \cdot \hat{\mathbf{n}}dl + \oint \left(\hat{\mathbf{k}} \times \mathbf{F}\right) \cdot \hat{\mathbf{n}}dl$$

Davis and Galarneau (2009)

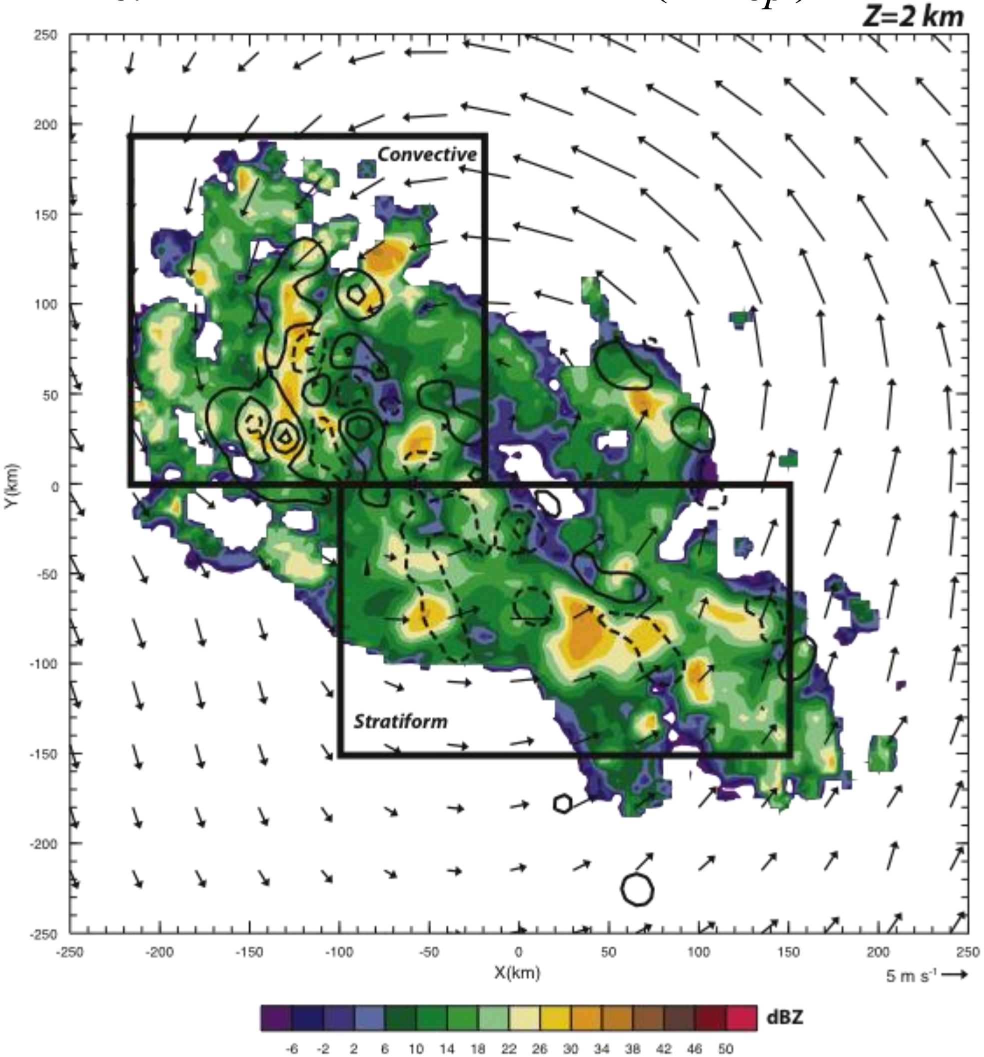

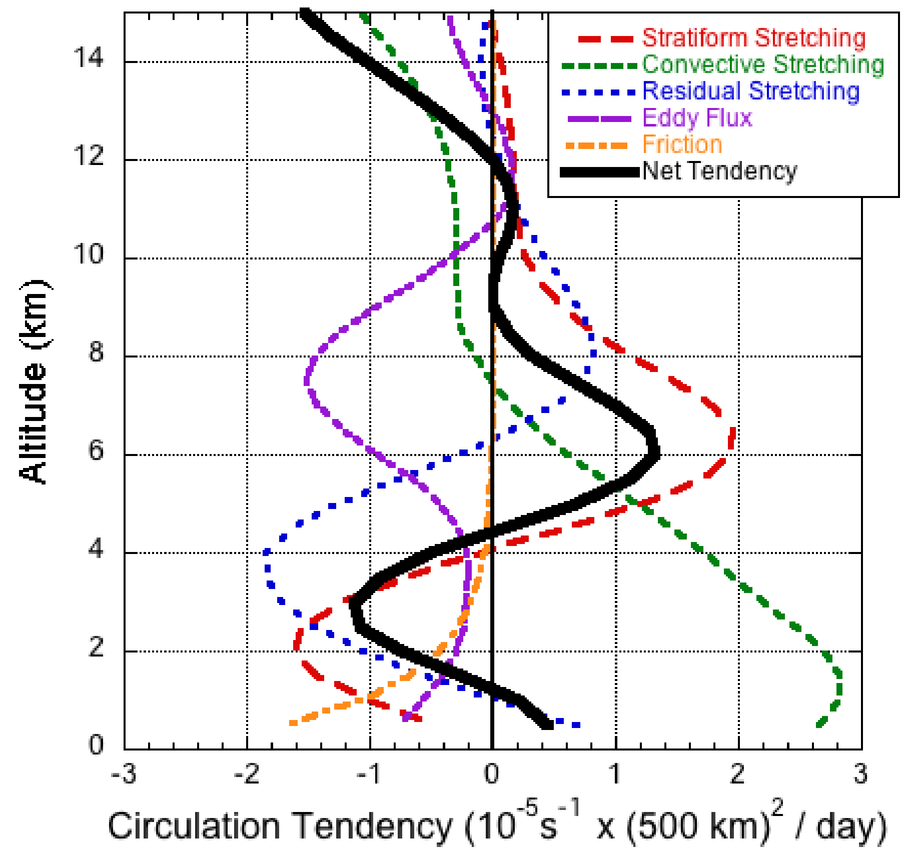

From Bell and Montgomery (2011)

SAMURAI analysis methodology

- 3DVAR system with cubic B-spline interpolations and quasi-spectral derivatives for vorticity and divergence
- Analyze dropsonde, flight level, satellite wind, and radar data in co-moving frame with ECMWF background
- Isotropic background error covariance with mass continuity constraint

$$q(r,z) = \left\{ \rho u, \rho v, \rho w, T', \rho_a', q_v', q_r' \right\}$$

$\bar{T}, \bar{\rho}_a, \bar{q}_v$ = Dunion (2011) Moist Tropical Sounding

SAMURAI analysis improves fidelity to PREDICT data

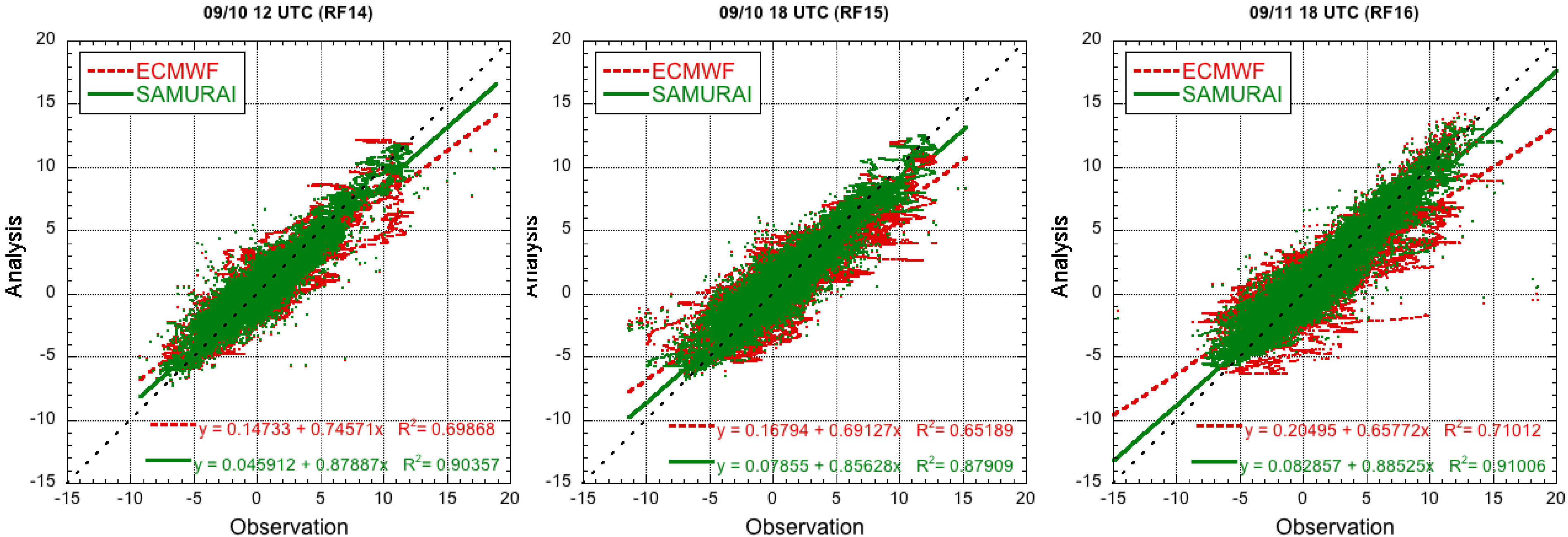

Variable	Background Error
pu, pv	5 (kg m^{-3}) * (m s^{-1})
pw	1 (kg m^{-3}) * (m s^{-1})
T'	3 K
p_a'	3 $x10^{-2}$ kg m^{-3}
q_v'	3 g kg^{-1}

12 UTC 10 September (RF14)

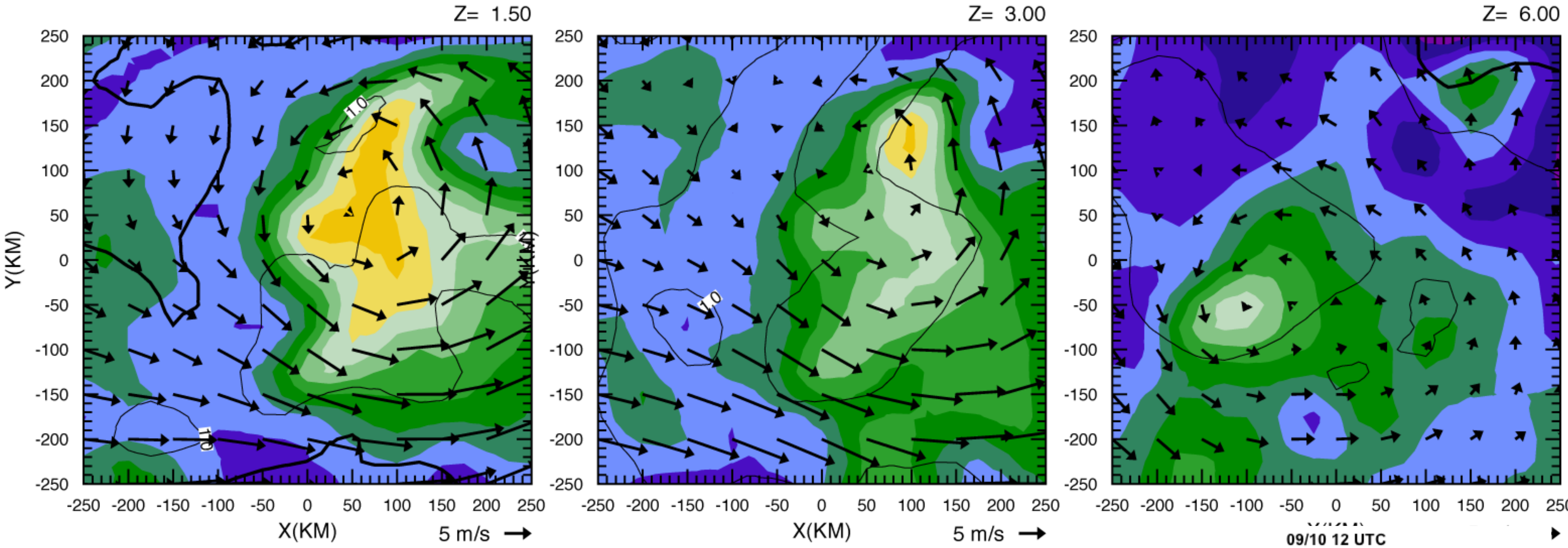

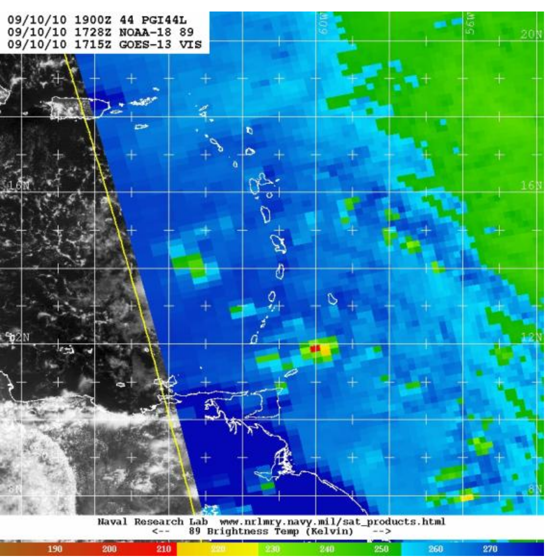

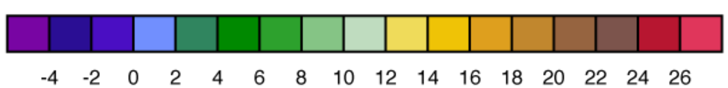

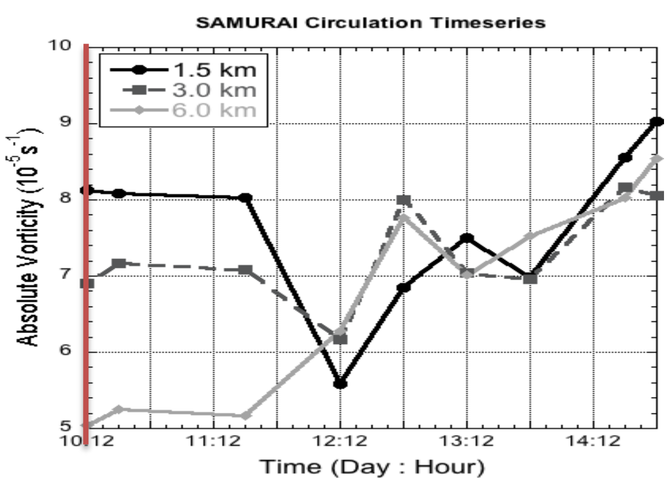

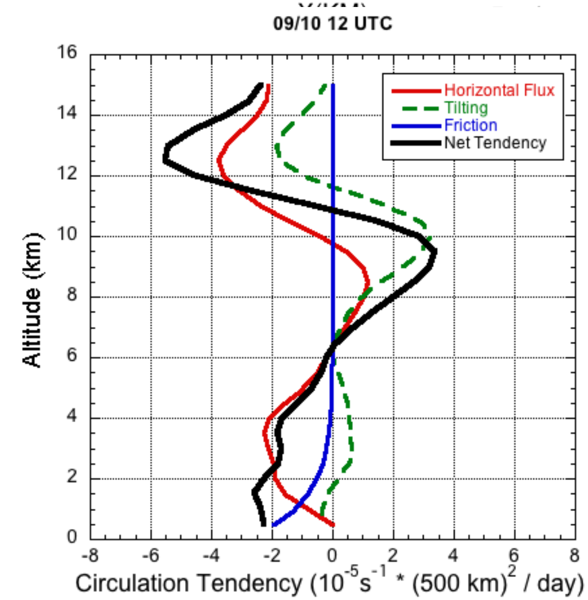

12 UTC 12 September (RF17)

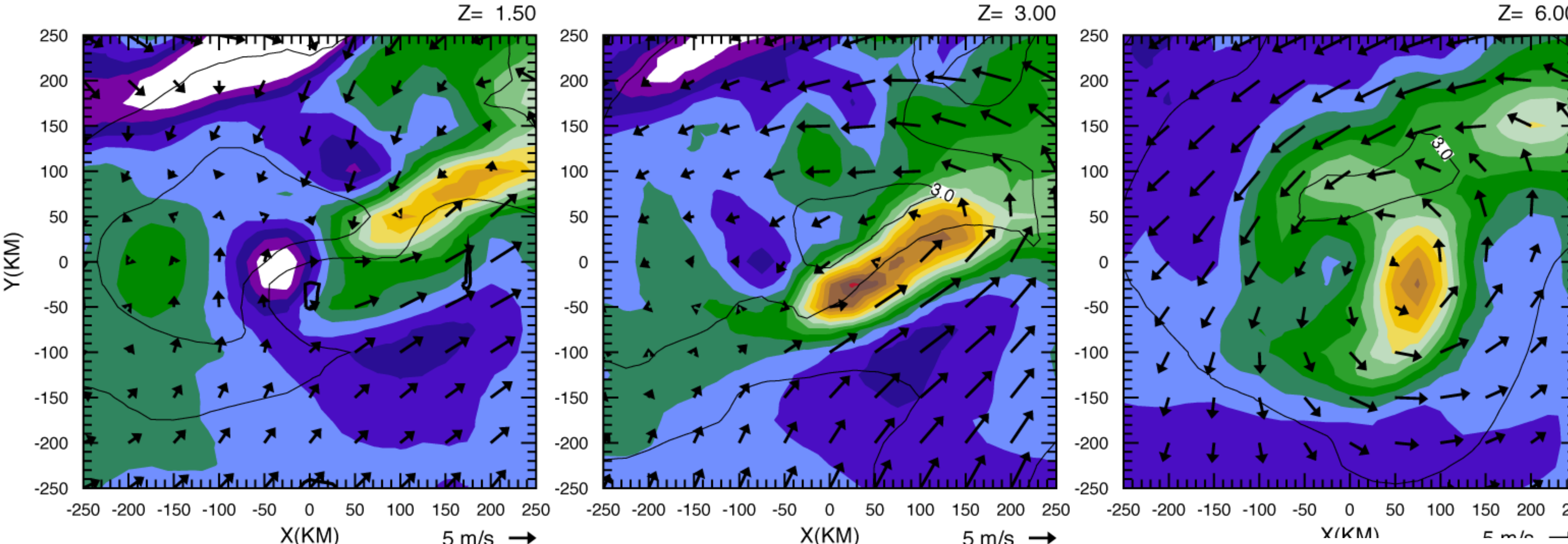

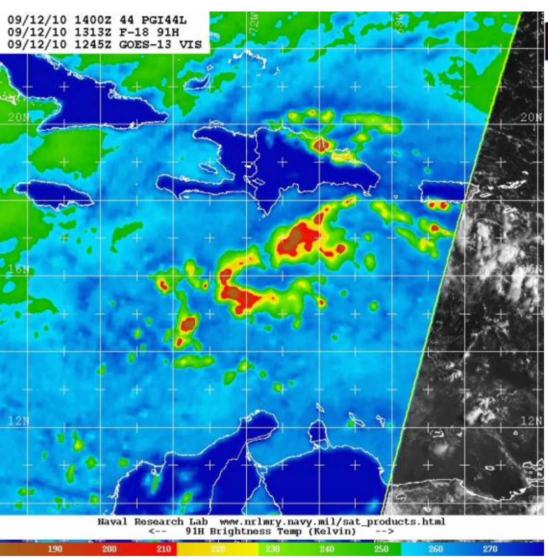

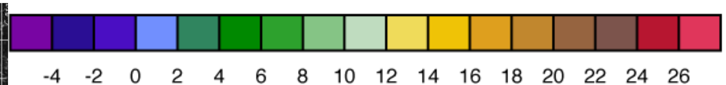

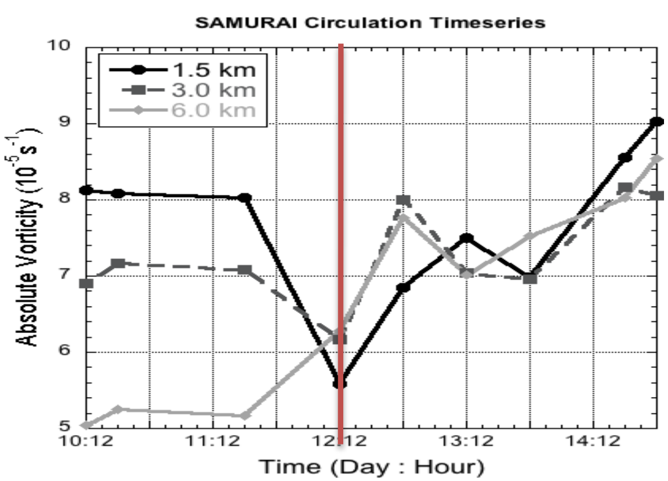

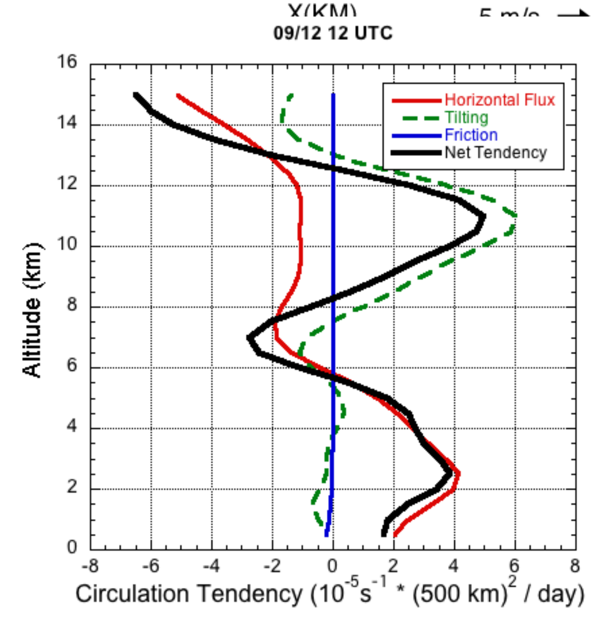

00 UTC 13 September (IFEX/GRIP)

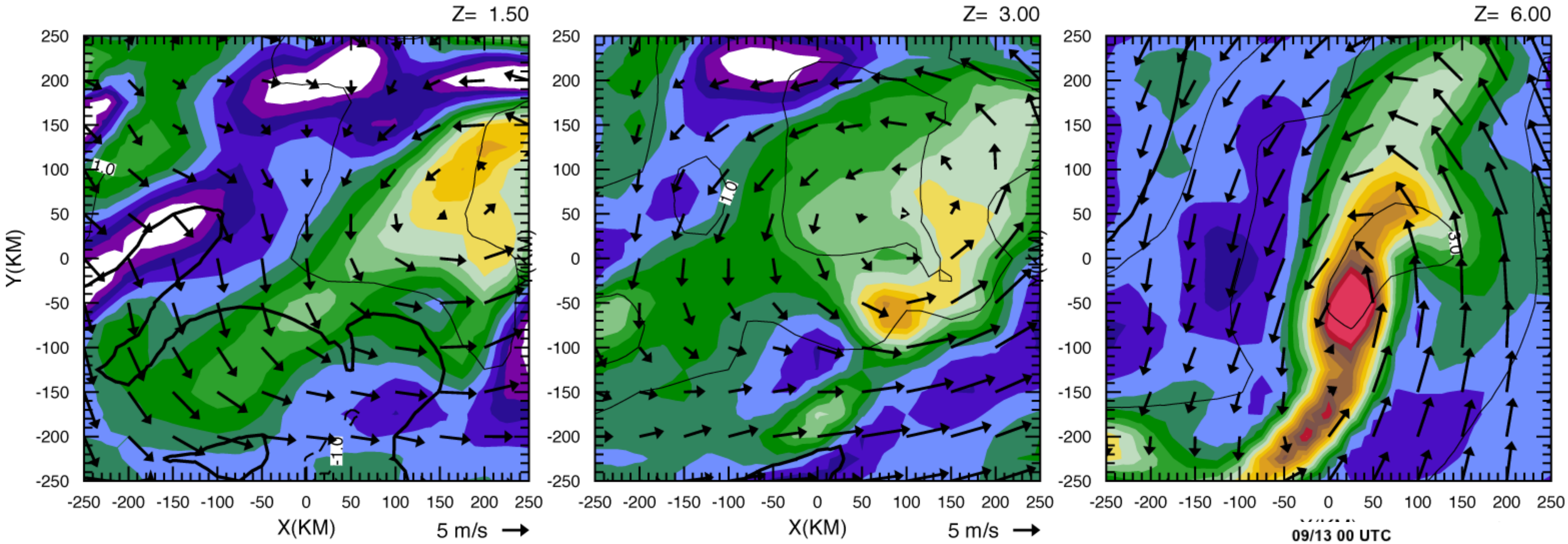

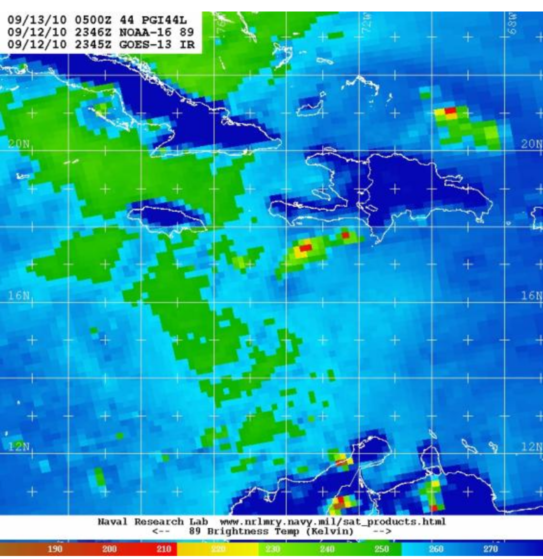

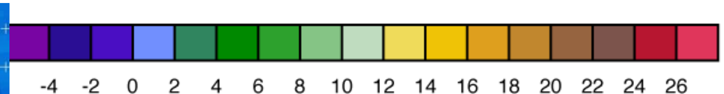

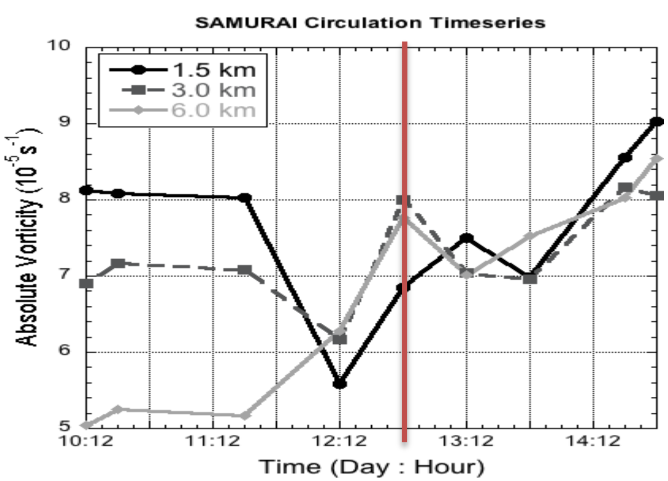

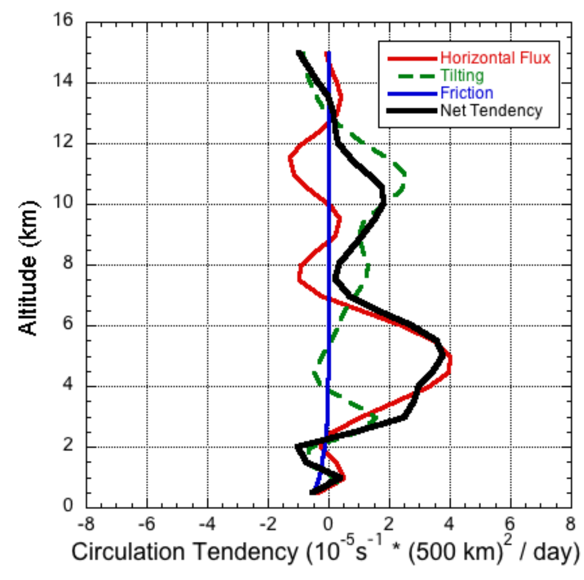

12 UTC 13 September (RF18)

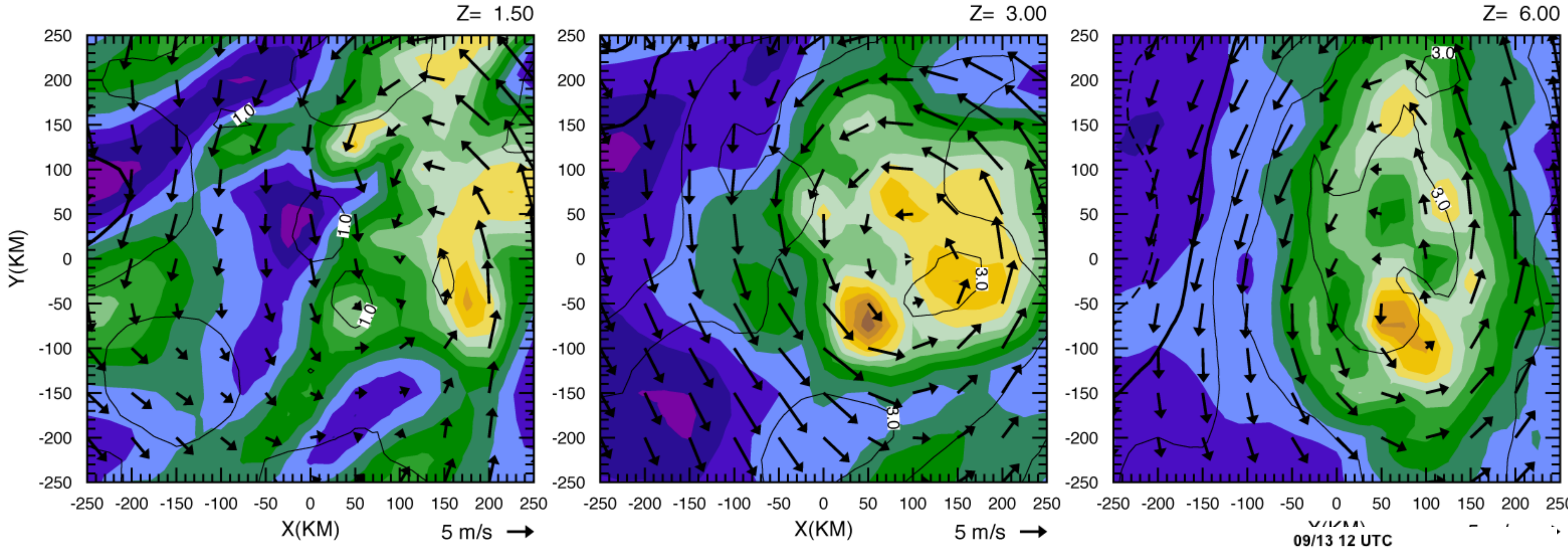

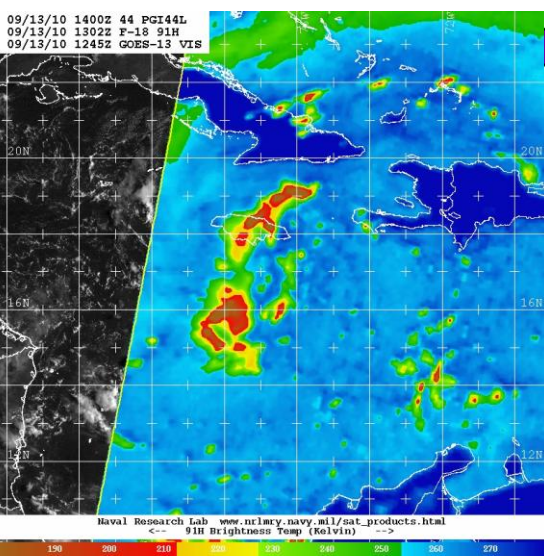

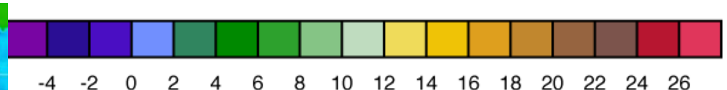

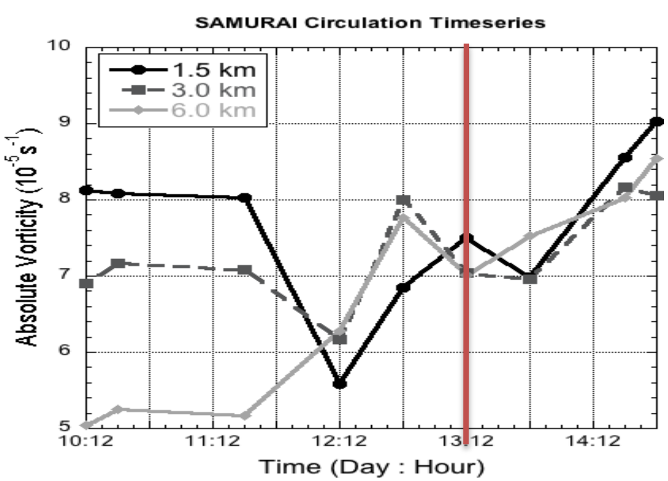

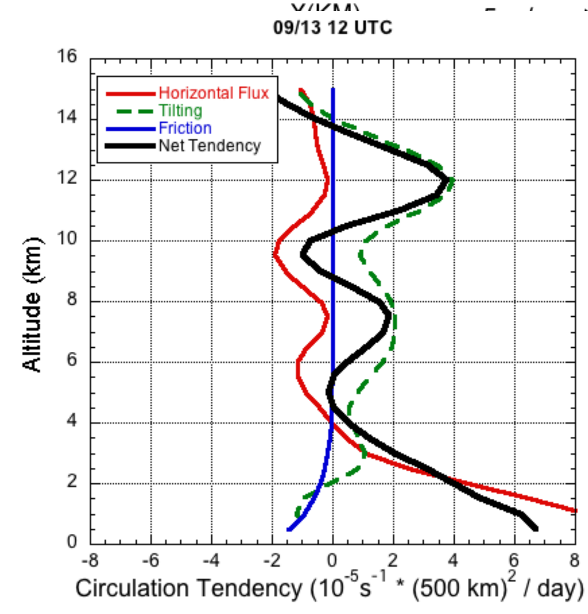

18 UTC 14 September (RF19)

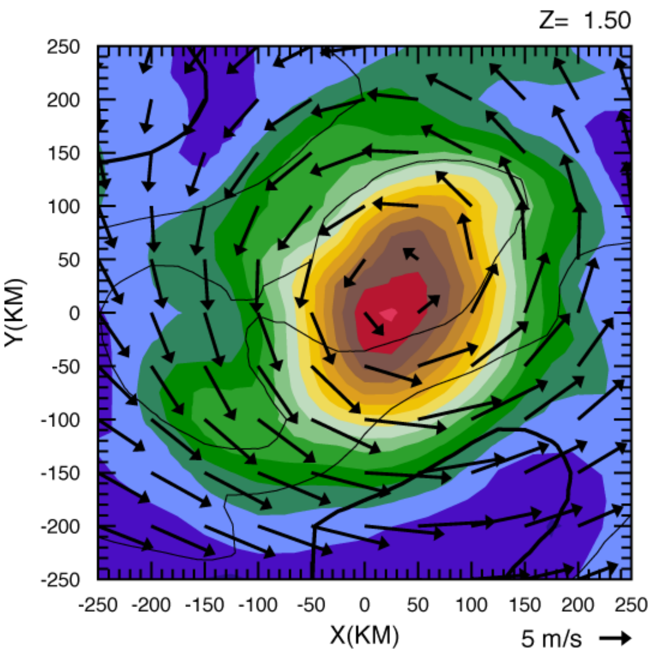

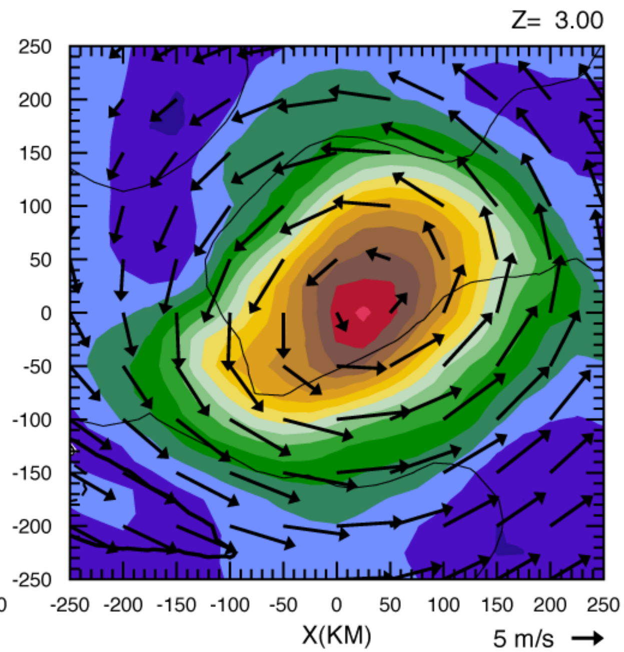

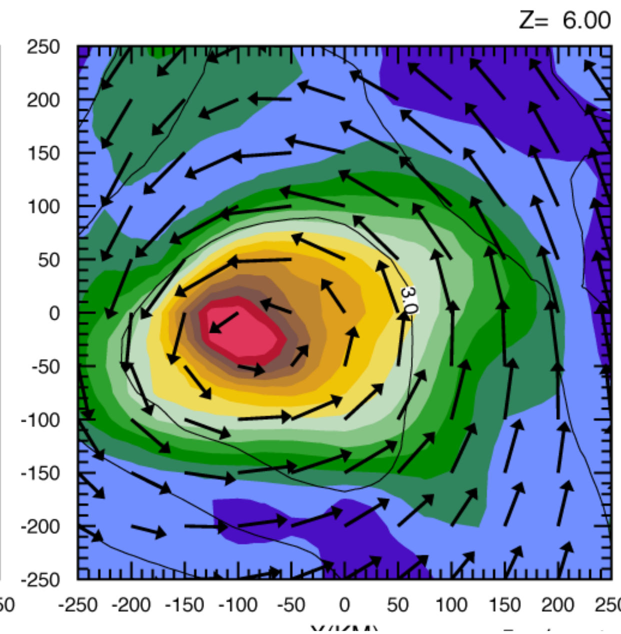

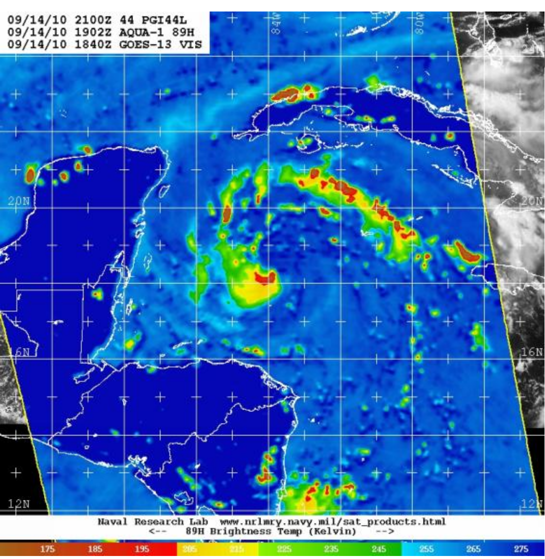

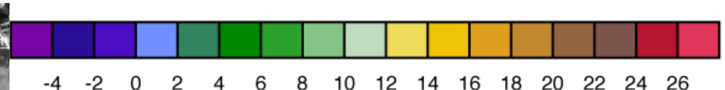

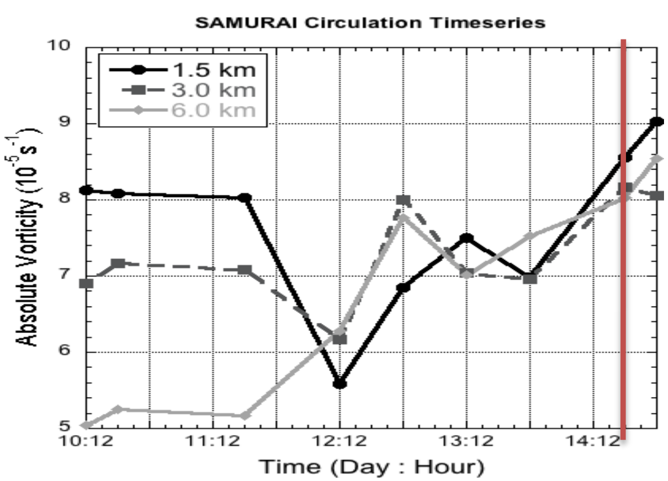

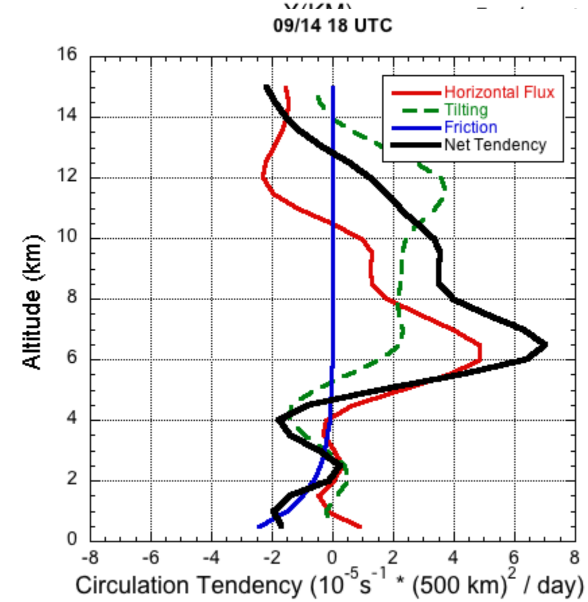

5 km analysis with NOAA Tail Radar

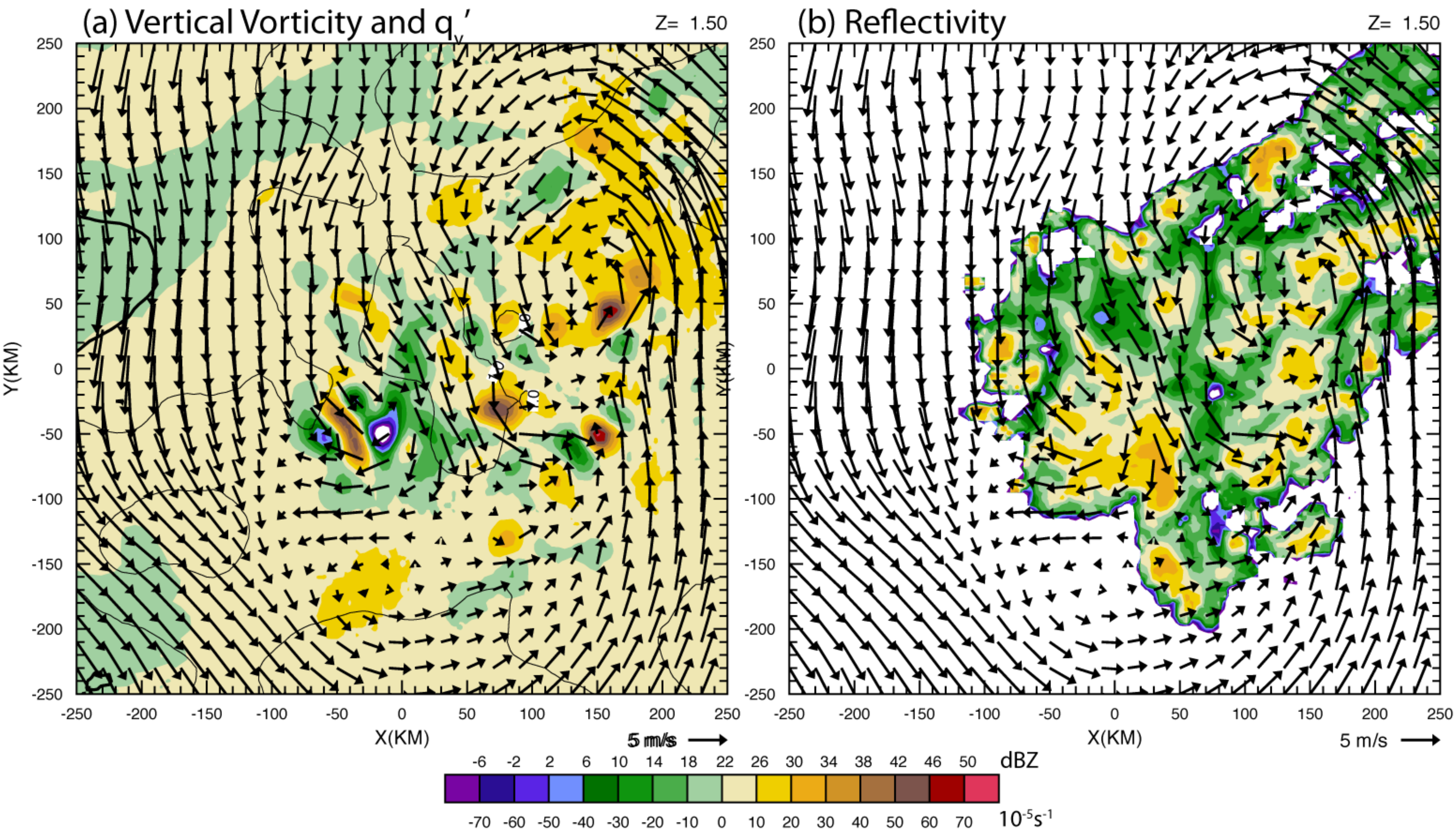

ysis with NOAA Tail Radar

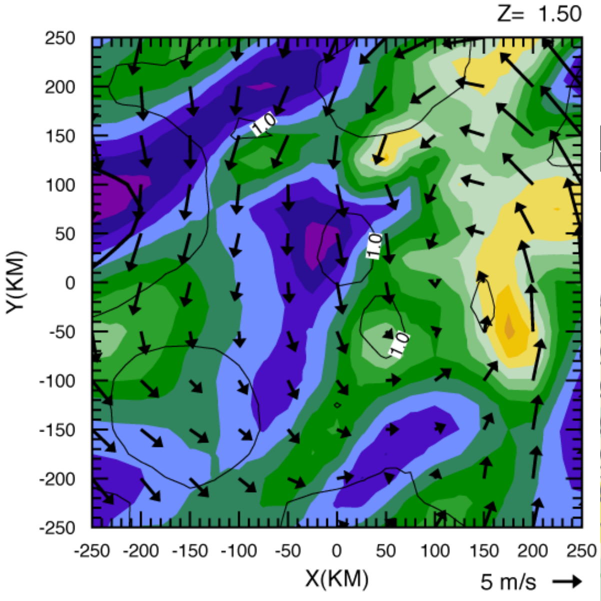

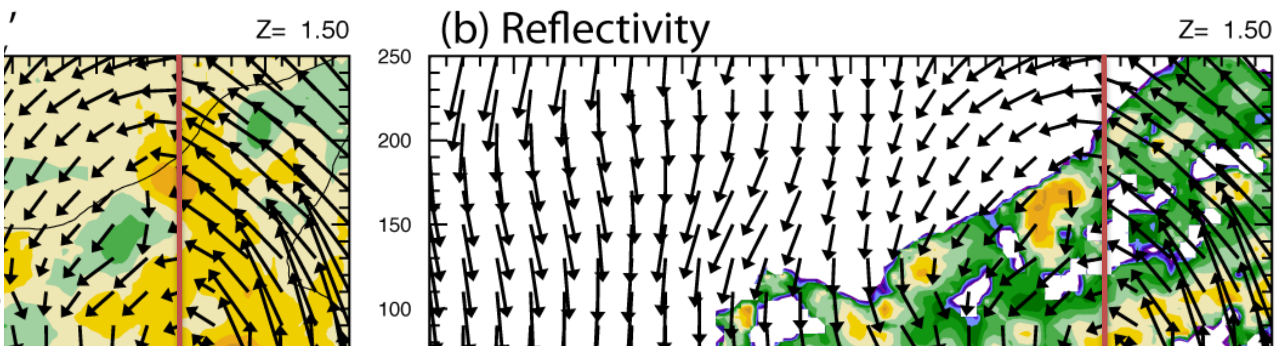
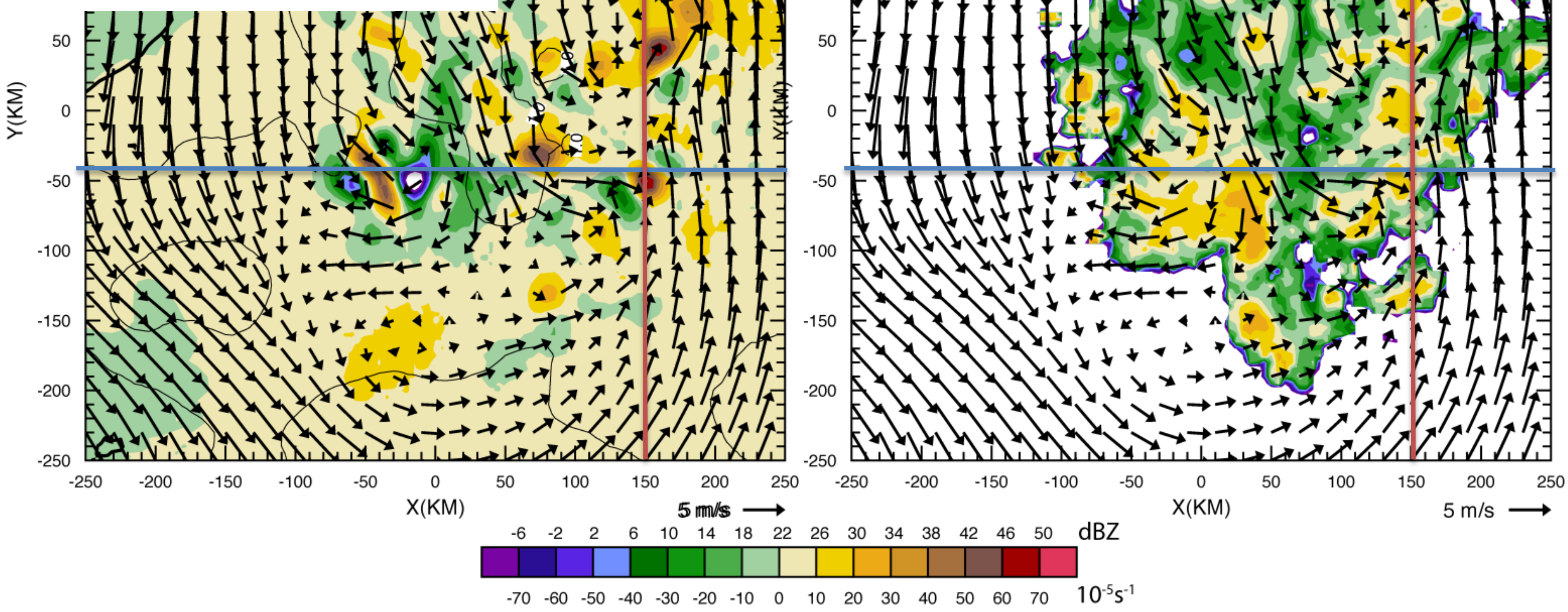

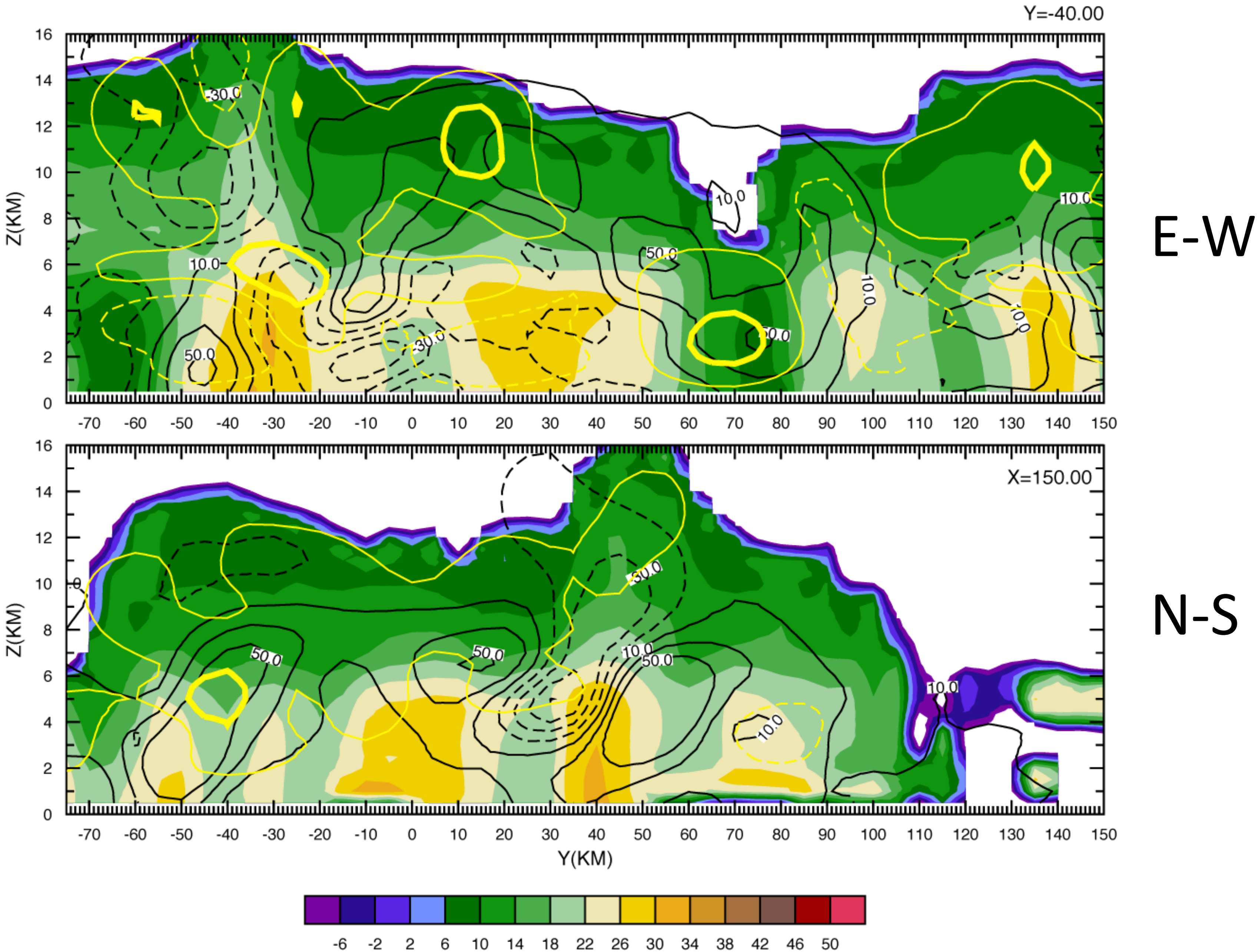
Y=-40.00
Z(KM)
E-W
X=150.00
N-S
Y(KM)
-6 -2 2 6 10 14 18 22 26 30 34 38 42 46 50

Preliminary Results Summary

- Successive convective bursts lead low-level spin-up and temporary decrease in moisture
- Mid-level spin-up and moisture recovery appear to follow bursts due to stratiform transition
- Preliminary radar data analysis shows a lot of structure!

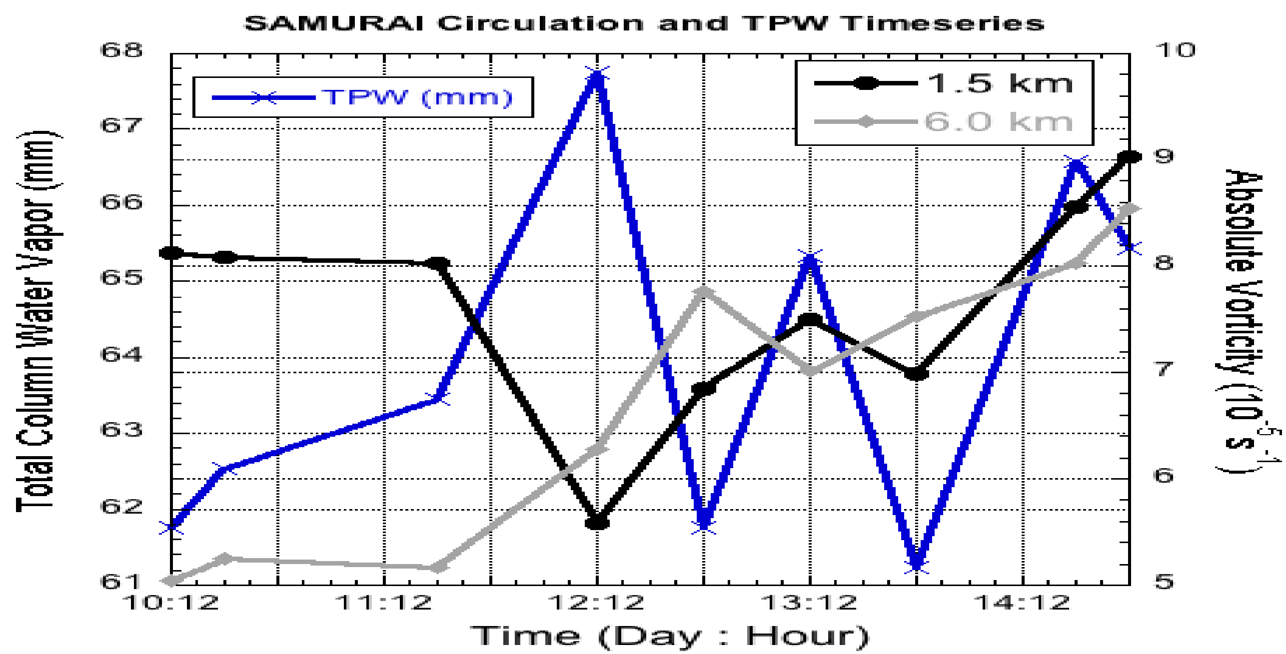

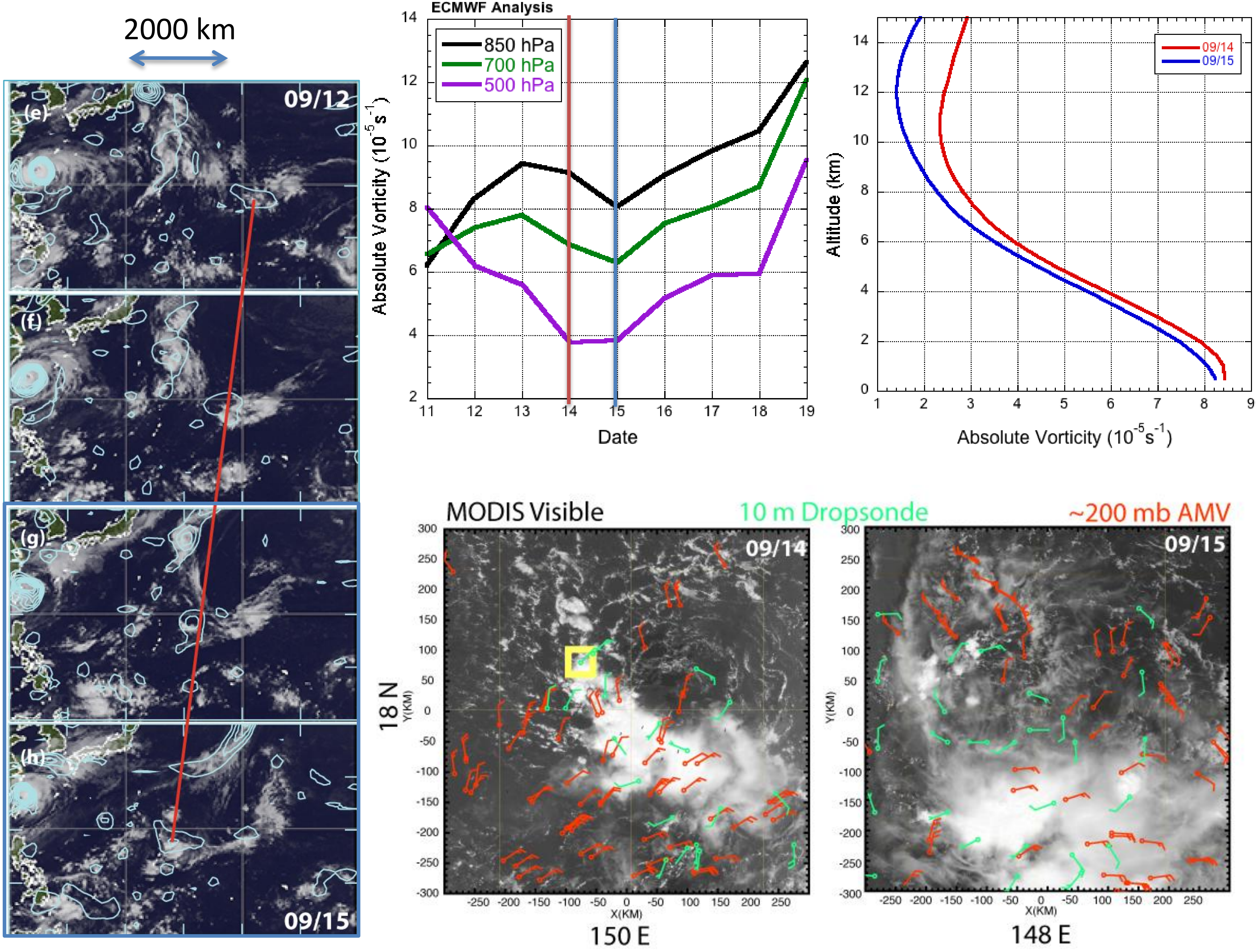

2000 km
(e)
09/12
(f)
(g)
(h)
09/15
ECMWF Analysis
850 hPa
700 hPa
500 hPa
Absolute Vorticity (10^{-5} s^{-1})
Date
09/14
09/15
Altitude (km)
Absolute Vorticity (10^{-5}s^{-1})
MODIS Visible
10 m Dropsonde
~200 mb AMV
09/14
09/15
18 N
Y(KM)
X(KM)
150 E
148 E